

Implication Of Geological Domains Data For Modeling And Estimating Resources From Nkout Iron Deposit (South-Cameroun)

Boroh Andre William (✉ williamboroh@gmail.com)

School Of Geology and Mining Engineering <https://orcid.org/0000-0001-7105-7301>

Sore-Gamo Koutou Yvan

School of Geology and Mining Engineering

Ayiwouo Ngounouno Mohamed

Ministry of Mines and Technology Development

Gbambié Mbowou Isaac Bertrand

School of Geology and Mining Engineering

Ngounouno Ismaïla

School of Geology and Mining Engineering

Research Article

Keywords: Information effect, support effect, geological domain, geochemical modelling.

Posted Date: March 19th, 2021

DOI: <https://doi.org/10.21203/rs.3.rs-270923/v1>

License:   This work is licensed under a Creative Commons Attribution 4.0 International License.

[Read Full License](#)

Abstract

This paper is devoted to determine whether the addition of geological information can improve the resource estimate of mineral resources. The geochemical data used come from 116 drill holes in the Nkout East iron deposit in southern Cameroon. These geochemical data are modeled on Surpac and Isatis softwares to represent the 3D geochemical distribution of iron in the deposit. Statistical analysis and then a variographic study is performed to study the spatial variability of iron. Estimation domains were defined based on the results of geological and geochemical analyses. Four domains were determined. These domains are in particular, the saprolitic domain; the poor domain or fresh rocks such as amphibolites, granites and gneisses; the rich domain or oxidized rocks (BIF) and the metasediment domain. Block modeling of the deposit is performed to estimate the resource. The grade of each block was estimated by using ordinary kriging and composites from each domain. This study also consisted of comparing two types of estimate, notably the domain estimate and the global estimate. The cross-validation made it possible to authenticate the obtained models. From this comparison, the domain estimation brings more precision the global estimate precisely on the error analysis while if we take into account the point clouds of the predicted and estimated values, the estimation by geochemical modelling provides the best results.

1. Introduction

The estimation of recoverable resources, on a global or local scale, has become a standard geostatistical application in the mining industry (Matheron, 1971). At the start of the analysis of the recoverable resource problem in the 1970s, both the support effect and the information effect were identified as playing a potentially important role in the result (Deraisme and Roth, 2000). To date, the support effect and the information effect are used significantly for writing estimate reports. Geostatisticians then resort to the notion of domain estimation (Rossi and Deutsch, 2014). On the one hand, the domains by geochemical grade are distinguished. The domain estimation involve the fragmentation of the deposit in intervals of regular or irregular grades for the estimation by making a correlation with the geology (Emery and Ortiz, 2005). On the other hand, the geological domains of a deposit are identified as a considerable support in the estimation of resources and their identification is an important step in the definition of the estimation domains for the quantification of a deposit because of the heterogeneity of the deposit (Ortiz et al., 2006; Kasmaee et al., 2019). Indeed, estimation domains can subsequently be modeled and used as a basis for geostatistical analyzes (Emery and al., 2007; Wilde and Deutsch, 2012), given that in geostatistics, the support is the physical size characterized by a geometry and an orientation, of the volume on which the regionalized variable Z is measured (Hocine et al., 2014). Glacken and Snowden have suggested that domain estimation is better than estimation without domain consideration (Glacken and Snowden, 2001), but this theory has been refuted by some studies which prove the opposite (Saito et al., 2005; Emery et al., 2007).

In the estimation of mineral resources, the identification of geological domains to be used for definition, modelling and estimation of these domains is a major concern. Generally, only the information effect is

taken into account, the support effect being often overlooked. The main objective of this paper is to judge the relevance of adding geological information in improving the estimate of deposits. More specifically, it is a question of identifying estimation domains from the geological domains of the deposit, of estimating the tonnage and of evaluating the quantity of metal of each domain in order to compare it with the global estimate without consideration of areas.

2. Geological Context Of The Study Area

The southern Cameroon area has given rise to a great deal of work and research, both geological and geomorphological (Gazel et al., 1956; Haugou and Koretzky, 1943; Korableff, 1940; Nicklès, 1952). The geological data of South Cameroon are extracted from documents and geological maps (Maurizot, 2000; Maurizot et al., 1986) modified by Lerouge (Lerouge et al., 2006) at 1: 200,000 (see Figure 1) available and published.

Our study area belongs to the lithostructural unit of lower Nyong which includes the greenstone belt (pyrogranites, pyroxeno-amphibolites, peridotites, garnetites, talcschists, quartzites and itabirites), the laminated series (gneiss, garnetite and amphibolites), plutonites (granodiorites and syenites) and doleritic veins. Pyroxenites, talcschists and amphibolites are believed to come from Archean greenstone belts belonging to the Nyong unit, the main beam of which is formed by the Mamelles - Mewongo - Ngovayang - Eséka alignment) (Lerouge et al., 2006; Vicat et al., 1998; Maurizot, 2000). The hydrothermal and meteoric aspect is respectively underlined by the presence of iron sulphides (pyrite, chalcopyrite, arsenopyrites) and chlorite. This NE-SW oriented unit rises to over 1000 m altitude and borders the Ntem group to the west. Geochronological studies give it a Paleoproterozoic age despite abundant relics. Archean and signs of Neoproterozoic rejuvenation. A quick recognition of the study area from Figure 1 shows that it consists of orthopyroxene gneisses, hornblende-Biotite gneisses and Neoproterozoic formations of the Yaoundé group. Petrostructural and geomorphological analyzes show that this region has been affected by three phases of deformation, the most important of which (the second) has set up tectonic units in mega synforms and antiforms (Gweth et al., 2001). The geological map of the study area is presented in Figure 1.

3. Definition Of Geological Estimation Domains

An in-depth phased approach has been developed. It is based on a combination of geological and geochemical analyses. This approach is more detailed and takes more time, but it provides a better support for the estimation because it is based on the decomposition of the problem by describing and modelling the geological layers and their geochemistry. The definition of the estimation domains begins with the geological knowledge of the area. It is therefore important to carry out a stratigraphic study first to observe the distribution of the lithological layers. These geological layers and their distributions are used as basic elements for the definition of the estimation domains. The next step is to study the variability of the iron content (%) in the boreholes. This is based on the geochemistry, overall abundance in the deposit, and information about the drill holes. A few litho-geochemical logs were thus modelled to

better observe the distribution of iron contents in the rocks and their arrangement in the area. Third, the estimation domains are based on all reasonable combinations of geological attributes and their grades. In order to automatically define the domains, a *Matlab code* has been written (see Appendix B). These domains are represented in Table 1.

Table 1: Lithology of estimation domains.

Lithology	Estimation domains	Code
Laterites	Saprolitic and lateritic domain	D1
Saprolites		
Gneiss	Poor domain	D2
Granite		
Pegmatite		
Magnetite BIF	Rich domain	D3
Hematite BIF		
Itabirites		
metasediments	Metasediments domain	D4
Quartzites and veins		
Schist		

- the saprolitic or lateritic domain (superficial layers). This domain is made up of laterites and surface layers. This zone is very rich in iron on the one hand (content up to 64%) and parts with variable contents depending on the degree of weathering of the rocks;
- the poor domain (group of granitic intrusions, pegmatites, amphibolites, gneiss): this domain is made up of fresh rocks which are amphibolites, granites, pegmatites and gneisses. Most of these rocks have low iron contents;
- the rich domain or domain of oxidized rocks (group of itabirites, BIF hematite and magnetite): BIF (hematites, magnetites) here contain high iron contents;
- the domain of metasediments (group of metasediments, schists and quartzites): metasediments and metasedimentary rocks in this domain have a low iron content. These rocks have undergone extensive metamorphism. Table 1 presents a summary of the estimation domains defined

4. Geochemical And Geological Modelling

4.1. Geochemical global domain

The iron geochemical model of Nkout East is presented in Figure 2.

This model represents the 3D geochemical distribution of iron in the deposit. Indeed, the drawn geological forms should be based on a sufficient amount of borehole information and other geological knowledge

which could include an ore deposit model, surface mapping, and structural and radiometric information. This type of model was created by the segment method while respecting the rules of modelling (Ostensen and Smits, 2002). The geochemical data was modeled on Surpac before being exported to Isatis for studies. The model obtained represents the iron content of the deposit. The volume of the geochemical model is 62 077 119 m³, the surface is 3 219 760 m².

4.2. Geological modelling of domains

The characteristics of this three-dimensional model of the fields of the deposit are established in Table 2 and Nkout East geological domain modeling is illustrated in Figure 3.

Table 2: Surface and volume of the geological model 3D.

	D1	D2	D3	D4	Total
Surface in m²	2 671 442	2 527 721	2 651 771	2 458 828	10 309 762
Volume in m³	14 921 078	39 037 962	50 231 970	41 593 959	145 784 969

A 3D geological model of the Nkout East deposit was built on the basis of drilling data and fields defined previously. Each model is representative of the rocks constituting the domain. Smoothing (see Figure 3) was then applied to the model to eliminate the rough surfaces associated with triangulation. The colorations observed on the model refer to the different fields. The saprolitic domain is found more on the surface.

5. Exploratory Data Analysis

The histogram of the iron composites of Nkout East over the entire deposit is given in Figure 4.

In Figure 4, it appears that this histogram follows a normal law with an average of 27.18% and a standard deviation of 19.86%. The coefficient of variation is 0.7237. The maximum value is 67.17% and the minimum value 0.48% . The histogram is unimodal and the lowest levels (0 to 10%) have the highest frequencies. Table 3 and Figure 5 give the statistical parameters and the histograms of the different geological domains modeled at Nkout East.

Table 3: Statistical parameters of iron grade.

Domains	Count	Minimum	Maximum	Mean	Standard deviation	Variation coefficient (σ/m)
Global	4816	0.48	67.17	27.18	19.67	0.7237
D1	4657	0.48	67.17	31.93	19.56	0.6126
D2	1508	0.59	40.18	4.860	6.018	1.238272
D3	1178	0.62	64.11	32.56	9.888	0.30369
D4	646	0.61	30.83	4.353	3.648	0.838043

Domain D1 has characteristics close to the total geochemical domain, in particular concerning the minimum and maximum and also the normal shape of its histogram. It is also the area with the lowest (0.67%) and highest (67.17%) grade.

Domain D2 and domain D4 present lognormal histograms (see Figures 5b and 5d) with the lowest contents and variances but also a large part of the data considered to be outliers (Surpac, 2013). These areas are considered uninteresting from a grade point of view.

Domain D3, judged to be the rich domain, has the best characteristics, in particular the largest average at 32.56% and the smallest correlation coefficient equal to 0.3 sign of the small dispersion of iron in the domain.

6. Variographic Analysis

Variographic analysis is performed to find the spatial correlation of the studied item (Antinao and Gosse, 2009; Chiles and Delfiner, 2009). A variogram map is a plot of experimental variogram values in a coordinate system (hx, hy) with the center of the map corresponding to the variogram at a shift of (0,0) (Gringarten et al., 1999). Its use makes it possible to determine the major directions of the mineralization then to construct variograms according to these directions. The primary variogram map of the total geochemical domain is shown in Figure 6.

In Figure 6, a major direction $N0^\circ$ of dip 70° . The 3D variogram extracted from this map as well as from the other secondary and tertiary variogram maps is given in Figure 7. This 3D variogram of geochemical domain is illustrated in Figure 7.

These variograms were calculated with a step of 100 m and an angular tolerance is 10° except for the vertical variogram, which uses a step of 20 m with an angular tolerance, is 5° because of the small thickness of the geochemical model. The three variograms have a spherical model. The pattern nugget effect is $0\%^2$ and the spherical component C is $280.90\%^2$. The lags are 132.1 m, 43.25 m and 43.25 m respectively. The variogram maps of structural analysis of geological domains are presented in Figure 8.

According to Figure 8, which show the structural analysis by geological domains. In domain D1, the variogram values vary from 0.10 to $466.76\%^2$. The primary variogram map obtained is quasi-isotropic

because it does not note any major variation in the value of variograms. However, the major direction chosen is N60E°.

The variogram map of domain D2 shows a variation between 0 and 148.48%². The major direction in the plane is N170°, large discontinuities in this area are observed. Thus, two variograms will be modeled, following the major direction of continuity N-19.9° dip - 1.7° and following the direction N 249.8° dip - 9.8° that represents the secondary direction of continuity. The variogram following the direction could not be calculated.

The rich domain (D3) clearly shows a preferential direction following the major direction of continuity N -159.6° dip - 22° and minor following the direction N 228.1° dip 41.6°. It also has the largest calculated theoretical variogram value.

Finally, the values of the variogram map of domain D4 vary from 0 to 66.37%² (See Figure 8d). The major direction of continuity in the plane is N 150°E. Thus, three variograms will be modeled, following the major direction of continuity N150E° (N-30°) and following the secondary direction N 240° E dip - 20° that represents the secondary direction of continuity and the vertical direction. The 3D variograms of geological domains is shown in Figure 9.

The variogram of domain D4 (see Figure 9d) is the only one that has a vertical component, because of the low thickness of the layers of the other domains. Figure 9a shows an omnidirectional variogram for domain D1. This choice was made because of the isotropy of its variogram map (see Figure 8). The Table 4 provides the characteristics of the variogram models.

Table 4 : Characteristics of variogram models for estimation.

Domain	Direction	Model	Nugget (% σ)	Range (m)	Sill (% σ)
D1	omnidirectionnal	Spherical	119.18	389.5 m	266.27
D2	N-19.9(-1.7°)	Spherical	23.90	301.9	80
	N249.8(-9.8°)	Spherical	23.90	1393	80
D3	N159.6(-22.5°)	Spherical	24.23	44.48	101.16
	N228.1°(41.6°)	Spherical	24.23	106.9	101.16
D4	N150	Spherical	8	700	38.51
	N240(-20°)	Spherical	8	400	38.51
	Vertical	Spherical	8		

7. Resource Estimation

It is an operation, which consists in determining the volume and tonnage values of the model blocks relating to each zone. The volume of the blocks is easily calculated knowing their dimensions.

- **Density analysis**

Figures 10 and 11 illustrate the density analyzes carried out first on the entire Nkout East deposit then on each subdivided domain.

The resource estimate takes into account the value of the density of the layers present in the area to be estimated. In the absence of a density compositing, it is important to find a density value corresponding to all the layers: this is done by a correlation via linear regression between the measured density values and the contents (Tercan et al., 2013). The equations obtained for the calculation of the density as a function of iron are linear in the form $y = ax + b$ where y is the density and x is iron. In all cases, the coefficient a is close to zero, which means that the iron has minimal impact on the density value: therefore, the value of b will be used. Table 5 presents the separation into domains allows us to appreciate the density values which correspond to the lithologies crossed.

Table 5: Density of domains.

Domain	Density
Geochemical	1.87
D1	1.93
D2	1.75
D3	2.37
D4	1.68

The highest density is that of the BIF domain and the lowest is the density of metasediments. The loss of information made during the overall estimation because the density obtained in this case is only close to that of domain D1.

- **Block modeling**

To facilitate resource estimation, block modeling of the deposit is performed. Different block sizes were chosen for each domain, these choices depend on the geometry of the geological / geochemical model, on the method of exploiting the spacing between the boreholes, on the compositing (Tercan et al., 2013). Using ordinary kriging and composites from each domain, the grade of each block was estimated. One of the most common approaches to obtaining the block estimate is to discretize a block at many points which are estimated using the point kriging approach. Then, the block grade can be obtained by averaging all of the individual point estimates in the block. This robust approach gives good results and is used in most specialized computer programs for mining geology applications (Abzalov, 2016).

The estimates were made with a minimum of 5 points and a maximum of 15 points. Figure 12 shows the block model of the total geochemical domain.

The number of sample blocks selected is 5570 units, or 25.87% of the model block. The contents vary between 0.38 and 64.41%. The average grade of the blocks is 22.66%. The standard deviation of kriging is 15.90%. With 3013 points used, the neighborhood search ellipsoid has the following characteristics:

- The radii of 272.42 m in X, 261.49 m in Y and 21.29 m in Z;
- Rotation of -5 ° along Z.

The block used to model domain 1 has 6016 sub-blocks. The estimated geochemical model is shown in Figure 13.

Figure 13 contains 4383 sample blocks that represent 72.86% of blocks. The iron content varies between 1.35% and 59.03%. The average content is 29.55% and the standard deviation is 14.65%. The richest blocks are located on the surface. About 4888 composite data were used; the neighborhood search ellipsoid has the following characteristics:

- The radius of 1045.46 m in X, 467.78 m in Y and 44.11 m in Z;
- Rotation of -5 ° along Z.

The block model of domain D2 is shown in Figure 14.

In Figure 14 domain D2 is consisted of 9758 sample blocks, after estimation, 544 sub-blocks have been preserved, ie 5.57%. The iron content varies between 1.61% and 31.84%. The average content is 7.03% and the standard deviation 4.50%. With 4089 points used, the neighborhood search ellipsoid has the following characteristics:

- The radius of 450 m in X, 250 m in Y and 100 m in Z;
- Rotation of -5 ° along Z.

The block used to model domain 3 is illustrated in Figure 15.

In Figure 15, the block model is consisted of 8177 sample blocks, after estimation, 724 sub-blocks have been retained, ie 8.85% (see Figure 15). The iron content ranges from 12.69% to 50.03%. The average content is 30.45% and the standard deviation 5.62%. With 3634 points used, the neighborhood search ellipsoid has the following characteristics:

- The radius of 1014.18 m in X, 581.12 m in Y and 31.67 m in Z;
- Rotation of -5 ° along Z.

The block model D4 is shown in Figure 16.

The model block of domain 4 has 7252 sample blocks, after estimation, 351 sub-blocks have been preserved, or 4.84%. The iron content ranges from 1.46% to 12.86%. The average content is 5.82% and the standard deviation is 2.75%.

- **Model authenticate: cross validation**

Determining the quality of a model involves its validation. One of the most used techniques is cross-validation (Browne, 2000; Westerhuis et al., 2008; Arlot et al., 2010). It is a process which from certain samples used to design the model, then re-estimate certain values of the output variable, this method involves the use of statistical parameters in order to diagnose the reliability as well as its associated parameters (Marko et al., 2014).

This reliability test was performed using Isatis software. It was a question of analyzing the global model first, then the models of domain estimation. This is a comparison graph between the true values and the estimated values. The more the points are concentrated on the bisector, the better the correlation. Figure 17 shows the cross-validation correlogram of the global model.

Thus for the overall estimate, the clouds are concentrated along the first bisector, which indicates good precision of the estimates with a high correlation coefficient equal to 0.98. The average of the errors is 0.02. The confidence level is 99%. The distribution is made along the bisector, therefore on all the data. For the analysis by geological estimation domains, the correlograms were constructed and presented in Figure 18

The results of the cross-validation comparison for all models are shown in Table 6.

Table 6: Comparison of the cross-validation parameters of the domain models and the global model.

	Global	Domain 1	Domain 2	Domain 3	Domain 4
Mean error	0.05	0.02	-0.03	0.03	-0.03
Variance error	17.36	12.18	12.55	12.045	7.898
variance of standardized errors	1.48	0.8358	0.8053	0.8043	0.8639
mean of the variances of the standardized errors	0.01	0	-0.01	0	-0.01

Variance of the standardized errors of the domains is closer to 1 than that of the overall model, so the estimate using the domains is more precise than the overall estimate. In addition, the variance of the estimation errors of the global model is higher (17.36%) than the domains (12.18%; 12.55%; 12.045% and 7.898% respectively), this proves that the models by domains are more robust than the global model, hence a better estimate.

For domain 1, the correlation cloud is very tight (figure 18a), which reflects a good correlation between the estimated data and the real data with a high coefficient equal to 0.98. The average of the errors is 0.02. The confidence level is 99%. The distribution is made all along the bisector because the contents of the

domain are distributed from 0 to more than 60% iron. This domain, made up of saprolites and laterites, is rich in iron but also has zones that have been altered, hence the variability of the grade.

For domain 2, the data are concentrated along the bisector towards the extreme left at the bottom (figure 18b). The correlation coefficient is 0.81. The mean of the errors is -0.03. This concentration shows us that this area is low content (average less than 10%). The rocks constituting this domain are fresh rocks such as gneisses, amphibolites, granites and pegmatites.

For domain 3, the data are grouped along the bisector in the center (figure 18c). The correlation coefficient is 0.87. The average of the errors is 0.03. This concentration in the center shows us that this area is rich (average greater than 30%), it is made up of oxidized rocks which are BIF (hematite and magnetite). Smaller values are greater than 10%.

For domain 4, the data are grouped along the bisector towards the extreme left at the bottom (figure 18d). The correlation coefficient is 0.82. The average of the errors is -0.02. this concentration shows that this area is very low in iron (average less than 6%). The maximum values do not exceed 22%.

8. Conclusion

This paper was devoted to estimate the mineral deposit of East Nkout (South Cameroon) by geological domain with that made by geochemical modeling and to compare to types of estimate. Statistical analysis and then a variographic study was performed to study the spatial variability of iron. The estimation models were then authenticated by cross-validation. On the one hand, the method by geochemical modeling gave a correlation coefficient of 98% while the modeling by geological domains provided as coefficient 98%, 81%, 87% and 82% for the domains D1, D2, D3 and D4 respectively. On the other hand, by studying estimation errors, it turns out that the second method studied provided better results. From the two techniques, it is very difficult to make a choice on which methodology to use for resource estimation.

Declarations

Funding

Not applicable

Conflicts of interest

We, the authors, declare that there is no conflict of interest related to this article

Availability of data and material

Data used for this article is confidential

Code availability

Not applicable

Ethics approval

Not applicable

Consent to participate

Not applicable

Consent for publication

Not applicable

References

Abzalov, M., 2016. Applied mining geology. Springer.

Antinao, J.L., Gosse, J., 2009. Large rockslides in the Southern Central Andes of Chile (32–34.5 S): Tectonic control and significance for Quaternary landscape evolution. *Geomorphology* 104, 117–133.

Arlot, S., Celisse, A., others, 2010. A survey of cross-validation procedures for model selection. *Stat. Surv.* 4, 40–79.

Browne, M.W., 2000. Cross-validation methods. *J. Math. Psychol.* 44, 108–132.

Chiles, J.-P., Delfiner, P., 2009. Geostatistics: modeling spatial uncertainty. John Wiley & Sons.

Emery, X., Ortiz, J., 2005. Estimation of mineral resources using grade domains: critical analysis and a suggested methodology. *J. South. Afr. Inst. Min. Metall.* 105, 247–255.

Emery, X., others, 2007. Probabilistic modelling of lithological domains and its application to resource evaluation. *J. South. Afr. Inst. Min. Metall.* 107, 803–809.

Gazel, J., Guiraudie, C., de Ribes, G.C., Hourcq, V., Nickles, M., Geologie, C.D. des M. et de la, 1956. Carte géologique du Cameroun. Direction des Mines et de la Geologie du Cameroun.

Glacken, I., Snowden, D., 2001. Mineral Resource Estimation By.

Gringarten, E., Deutsch, C., others, 1999. Methodology for variogram interpretation and modeling for improved reservoir characterization, in: *Spe Annual Technical Conference and Exhibition*. Society of Petroleum Engineers.

Gweth, P.N., Dupuy, J., Matip, O., Fombutu, A., Kalngui, E., 2001. Mineral resources of Cameroon. SOPECAM Yaoundé 375.

Haugou, P., Koretzky, N., 1943. Carte géologique du Cameroun n 3 à 1/500.000 avec notice explicative. Serv Mines Cameroun Yaoundé.

Hocine, M., Balakrishnan, N., Colton, T., Everitt, B., Piegorisch, W., Ruggeri, F., Teugels, J., 2014. Wiley statsref: Statistics reference online. John Wiley & Sons, Ltd.

Kasmaee, S., Raspa, G., de Fouquet, C., Tinti, F., Bonduà, S., Bruno, R., 2019. Geostatistical Estimation of Multi-Domain Deposits with Transitional Boundaries: A Sensitivity Study for the Sechahun Iron Mine. *Minerals* 9, 115.

Korableff, G., 1940. Contribution à l'étude de la géologie et de la géologie appliquée de l'Oubangui-Chari oriental et du Cameroun sous mandat français. Libr. sociale et économique.

Lerouge, C., Cocherie, A., Toteu, S.F., Penaye, J., Milési, J.-P., Tchameni, R., Nsifa, E.N., Fanning, C.M., Deloule, E., 2006. Shrimp U–Pb zircon age evidence for Paleoproterozoic sedimentation and 2.05 Ga syntectonic plutonism in the Nyong Group, South-Western Cameroon: consequences for the Eburnean–Transamazonian belt of NE Brazil and Central Africa. *J. Afr. Earth Sci.* 44, 413–427.

Marko, K., Al-Amri, N.S., Elfeki, A.M., 2014. Geostatistical analysis using GIS for mapping groundwater quality: case study in the recharge area of Wadi Usfan, western Saudi Arabia. *Arab. J. Geosci.* 7, 5239–5252.

Maurizot, P., 2000. Carte géologique du sud-ouest Cameroun. Échelle 1/50 000.

Maurizot, P., Abessolo, A., Feybesse, J., Johan, V., Lecomte, P., 1986. Etude et prospection minière du Sud-Ouest Cameroun. Synthèse des travaux de 1978 à 1985. Rapp. BRGM 85 CMR 66, 274p.

Nicklès, M., 1952. Mollusques du Quaternaire marin de Port-Gentil (Gabon). *Bull. Dir. Mines Géologie LAEF* 5, 75–101.

Ortiz, X., others, 2006. Geostatistical estimation of mineral resources with soft geological boundaries: a comparative study. *J. South. Afr. Inst. Min. Metall.* 106, 577–584.

Rossi, M.E., Deutsch, C.V., 2014. Recoverable Resources: Estimation, in: *Mineral Resource Estimation*. Springer, pp. 133–150.

Saito, H., McKenna, S.A., Zimmerman, D.A., Coburn, T.C., 2005. Geostatistical interpolation of object counts collected from multiple strip transects: Ordinary kriging versus finite domain kriging. *Stoch. Environ. Res. Risk Assess.* 19, 71–85. <https://doi.org/10.1007/s00477-004-0207-3>

Surpac, G., 2013. 6.6. 1.(2013). GEOVIA Surpac Ref. Man.

Tercan, A.E., Ünver, B., Hindistan, M.A., Ertunç, G., Atalay, F., Ünal, S., Killoğlu, Y., 2013. Seam modeling and resource estimation in the coalfields of western Anatolia. *Int. J. Coal Geol.* 112, 94–106.

Vicat, J.-P., Pouclet, A., Nsifa, E., 1998. Les Dolérites du Groupe du Ntem (Sud Cameroun) et des Régions Voisines (Centrafrique, Gabon, Congo, Bas Zaïre): Caractéristiques Géochimiques et Place dans l'Évolution du Craton du Congo au Protérozoïque. *Géologie Environ. Au Cameroun Collect. GEOCAM* 305–324.

Westerhuis, J.A., Hoefsloot, H.C., Smit, S., Vis, D.J., Smilde, A.K., van Velzen, E.J., van Duijnhoven, J.P., van Dorsten, F.A., 2008. Assessment of PLS-DA cross validation. *Metabolomics* 4, 81–89.

Wilde, B.J., Deutsch, C.V., 2012. Kriging and Simulation in Presence of Stationary Domains: Developments in Boundary Modeling, in: Abrahamsen, P., Hauge, R., Kolbjørnsen, O. (Eds.), *Geostatistics Oslo 2012*. Springer Netherlands, Dordrecht, pp. 289–300. https://doi.org/10.1007/978-94-007-4153-9_23

Figures

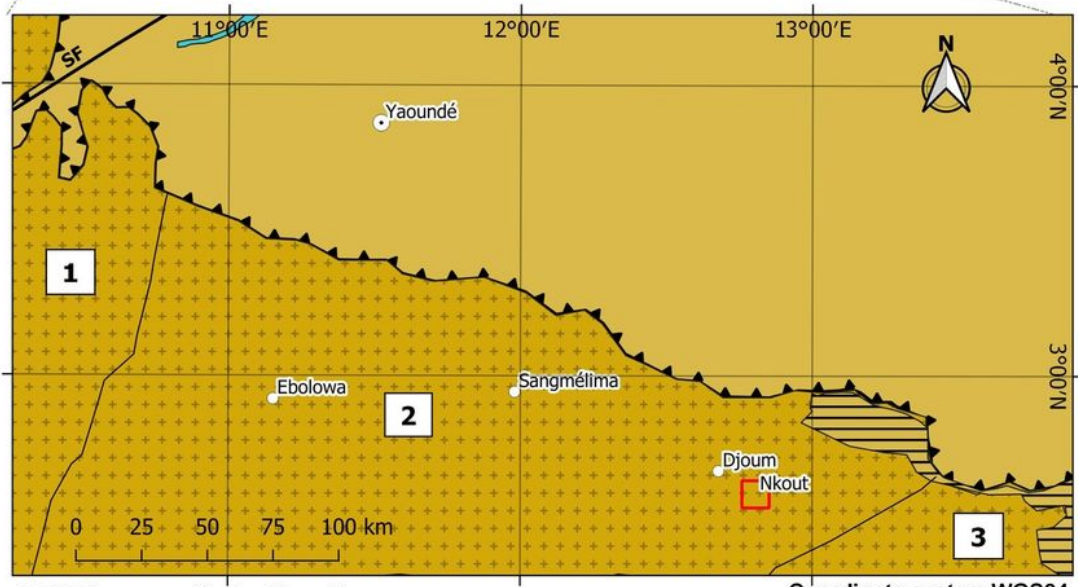
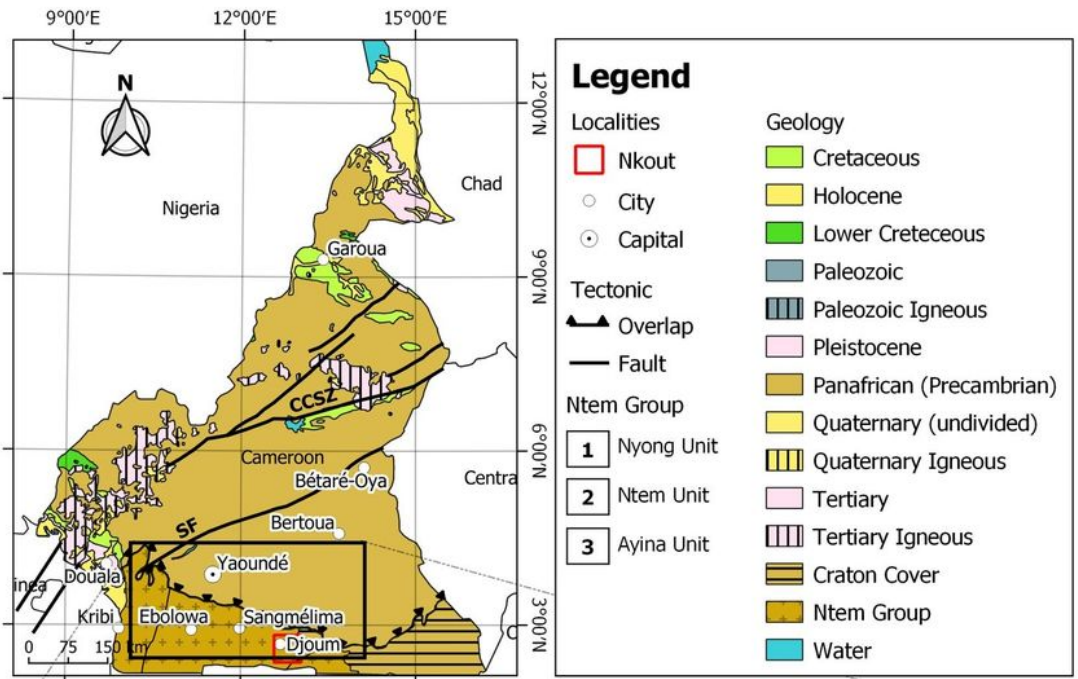


Figure 1

Local geology of Cameroon (modified from (Vicat, 1998)).

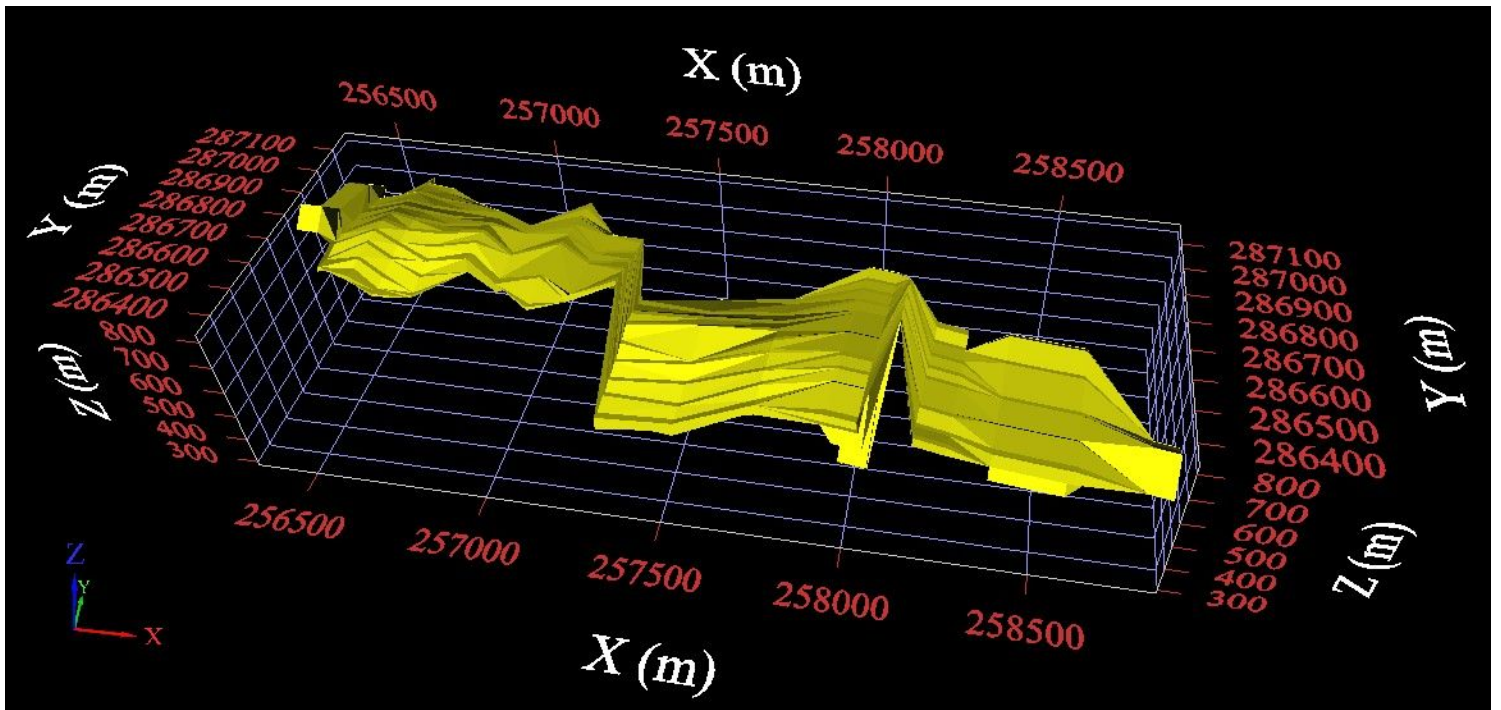


Figure 2

Iron geochemical model of Nkout East.

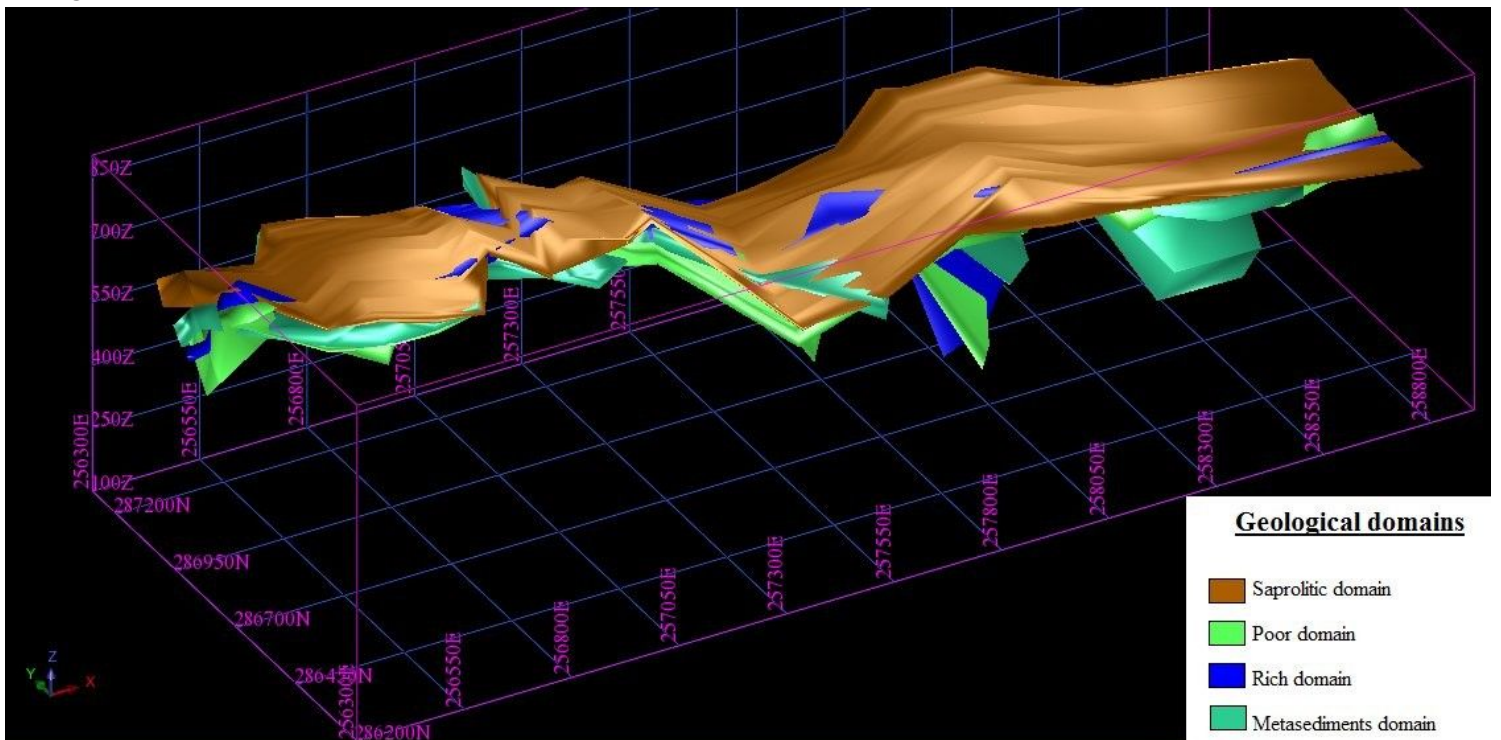


Figure 3

Nkout East geological domain modeling smoothed.

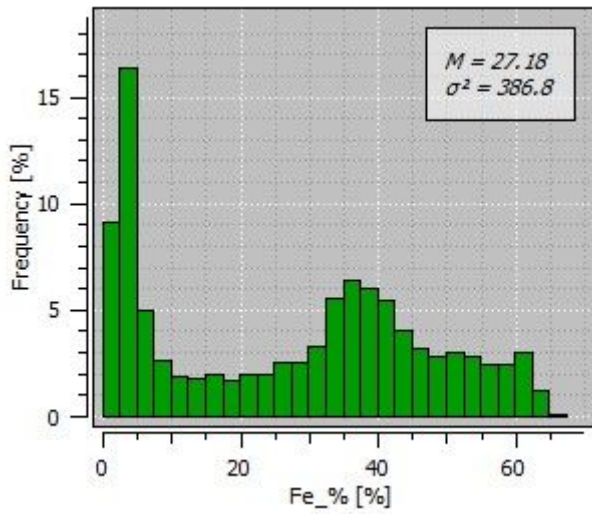


Figure 4

Histogram of iron grade of Nkout East.

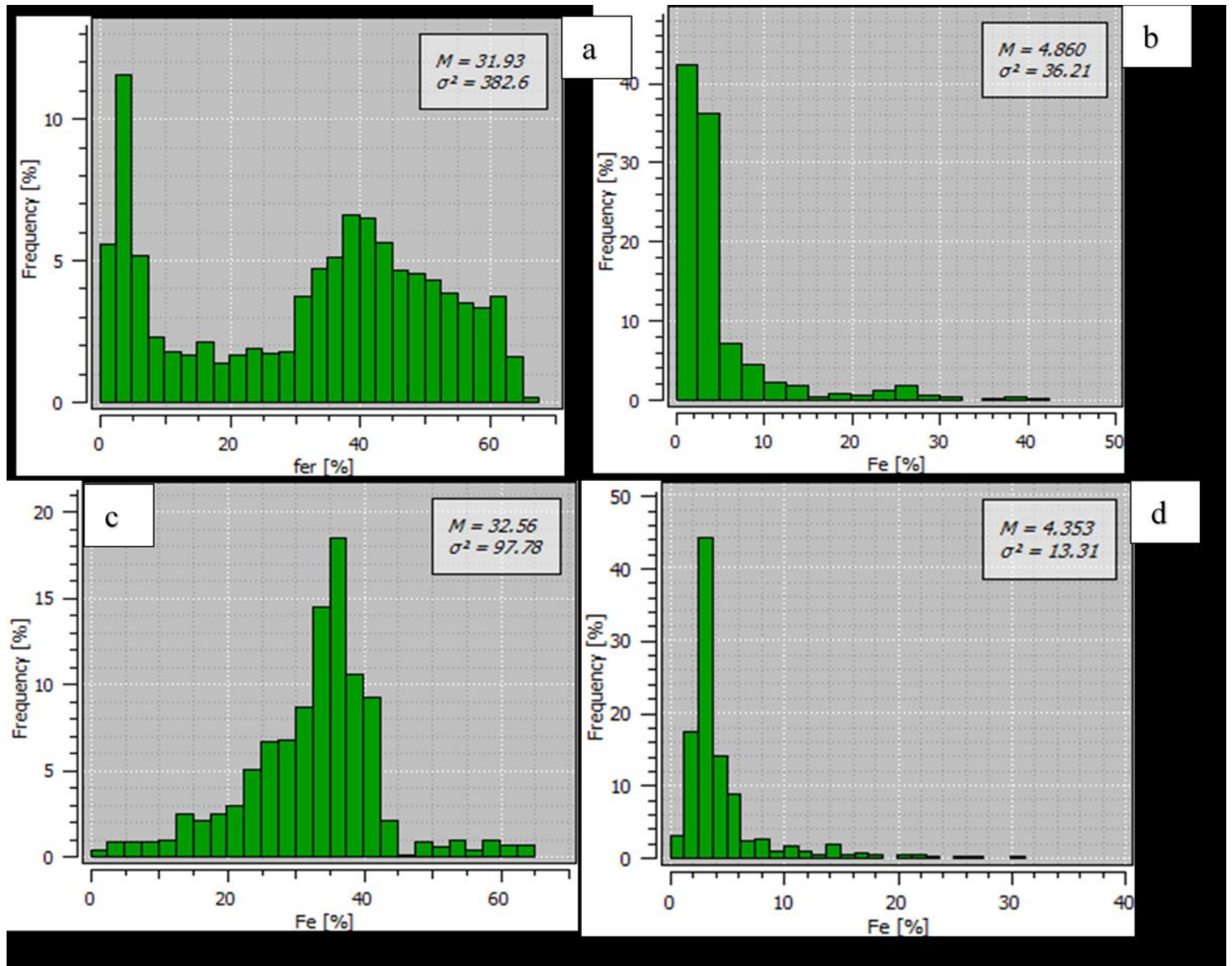


Figure 5

Histograms of iron grades by domains: a) D1; b) D2; c) D3 and d) D4.

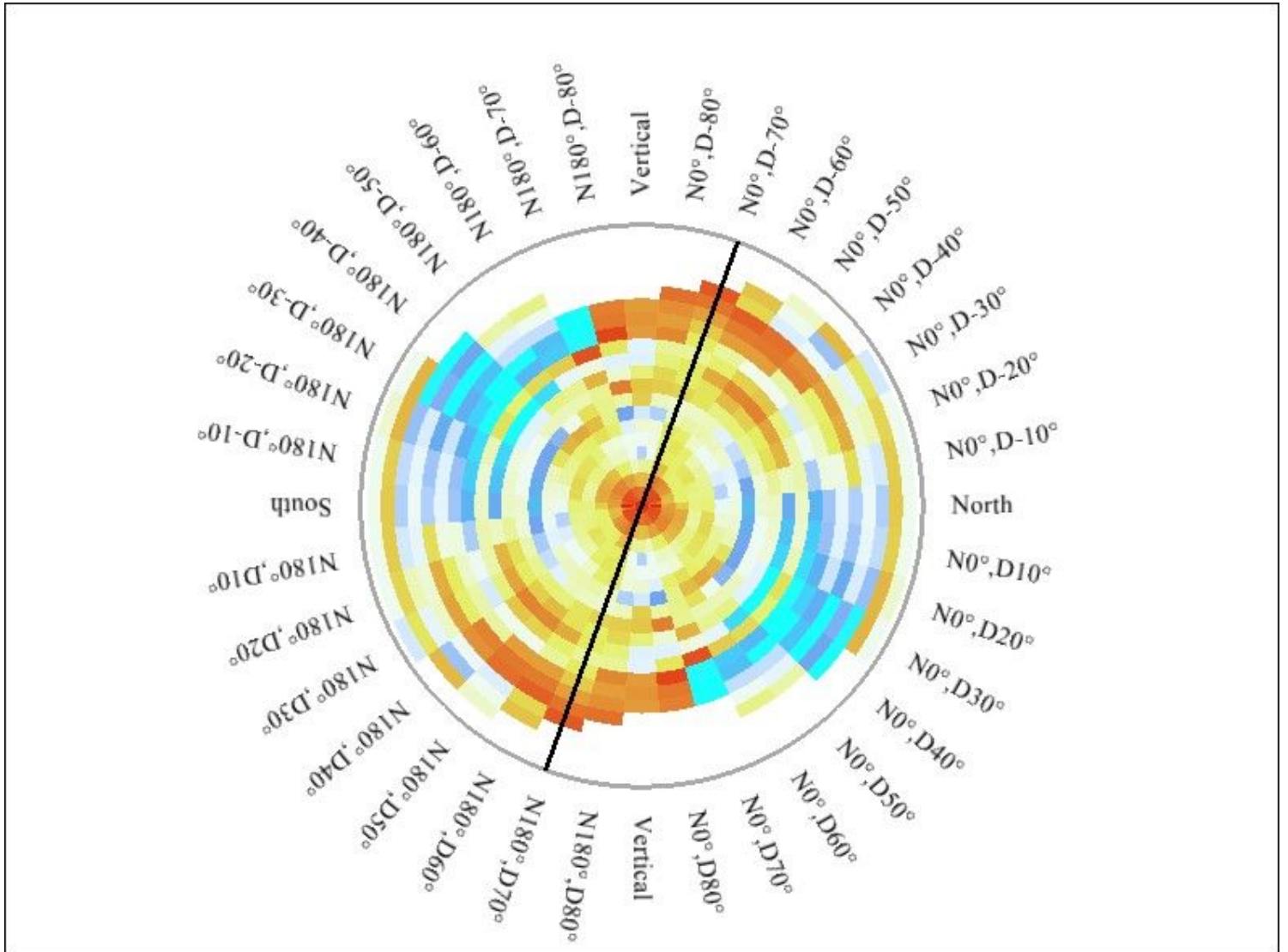


Figure 6

Variogram map of geochemical domain.

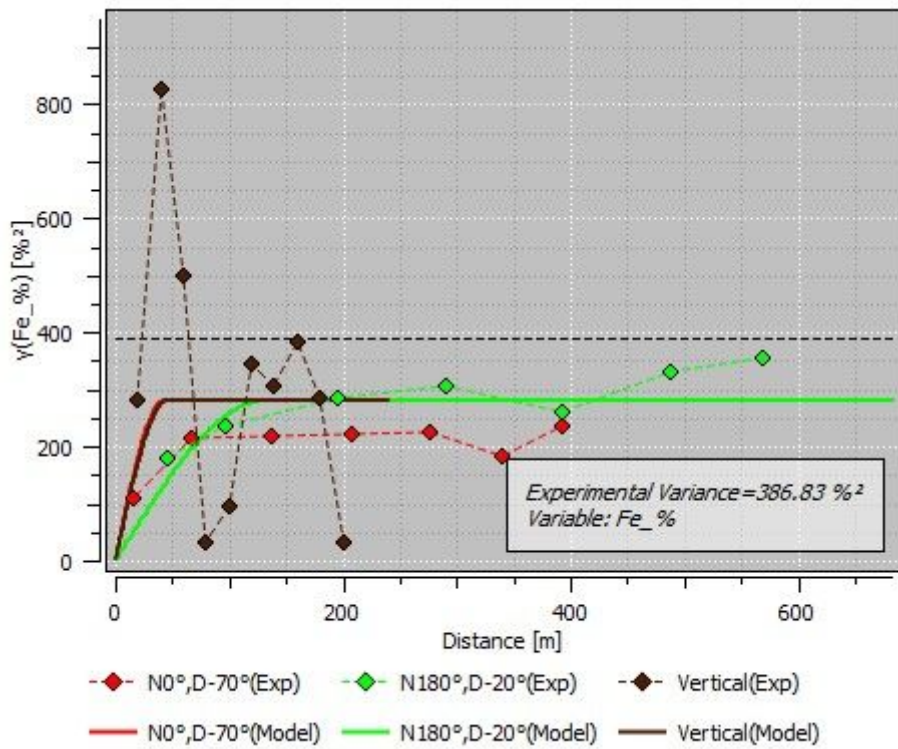


Figure 7

3D variogram of geochemical domains.

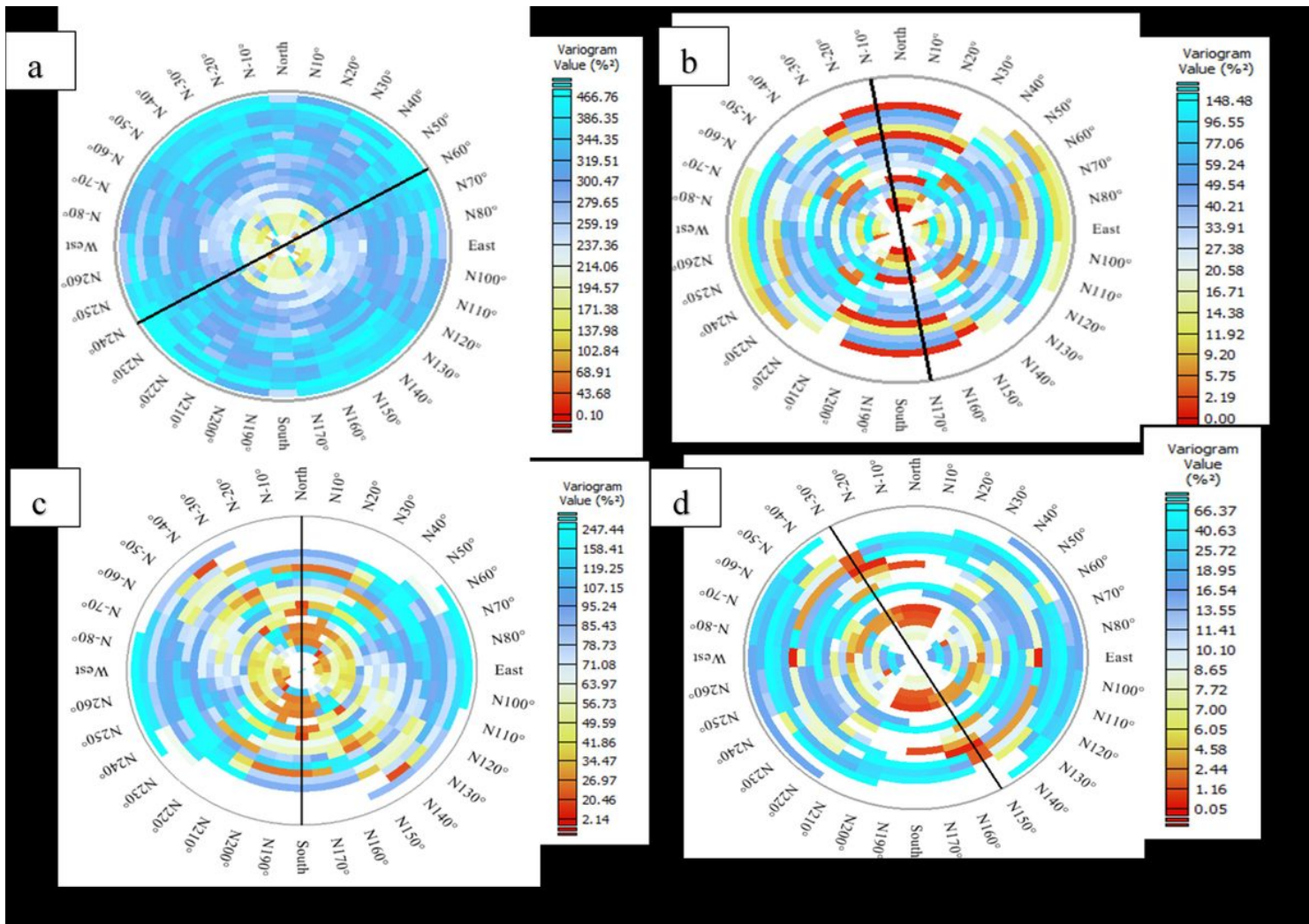


Figure 8

Variogram maps of geological domains: a) D1; b) D2; c) D3 and d) D4.

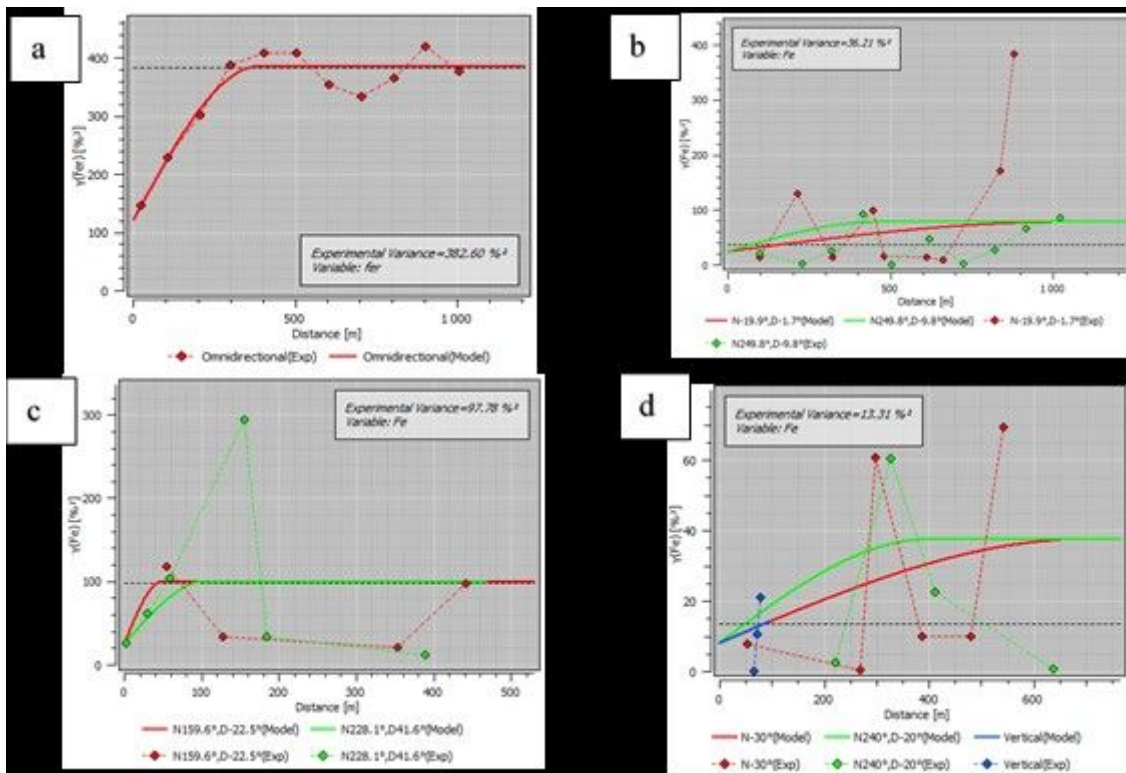


Figure 9

3D variograms of geological domains: a) D1; b) D2; c) D3 and d) D4.

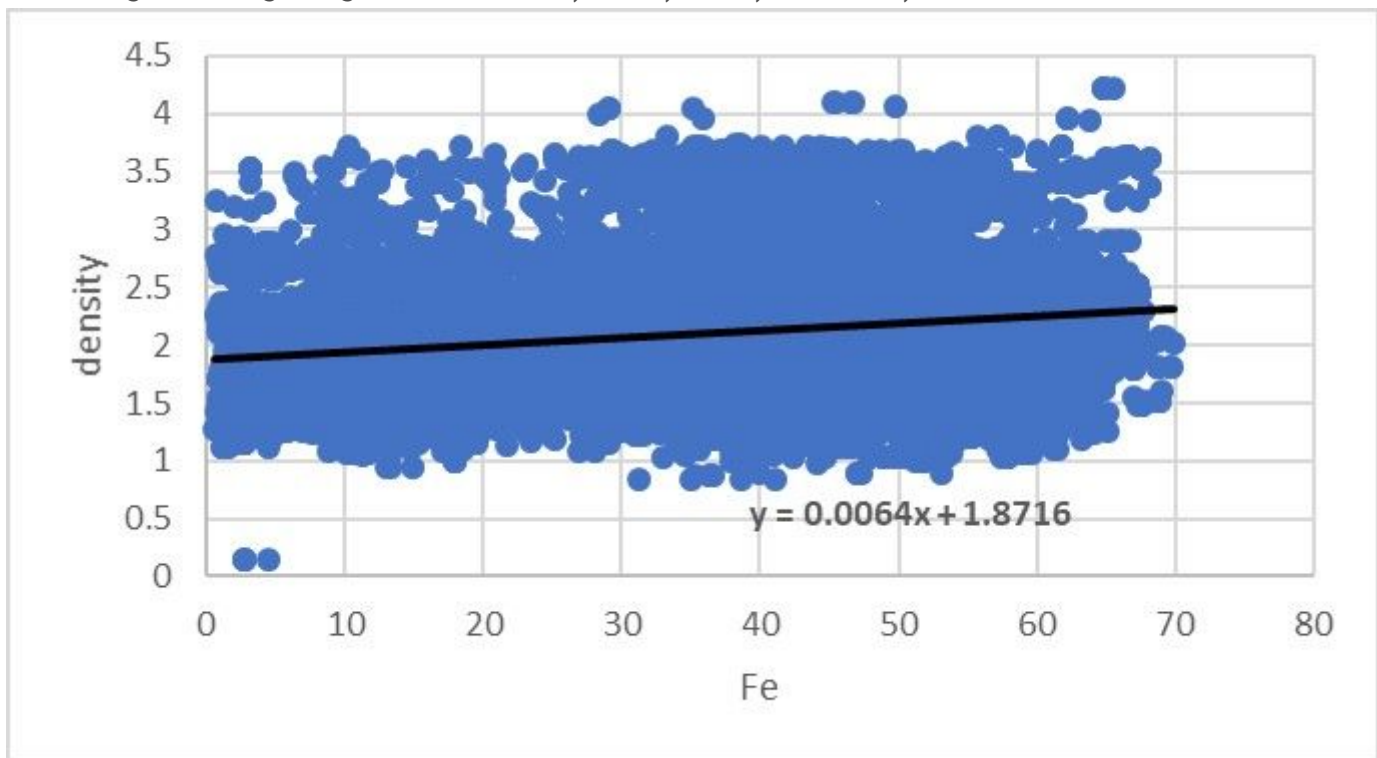


Figure 10

Density analysis Nkout East.

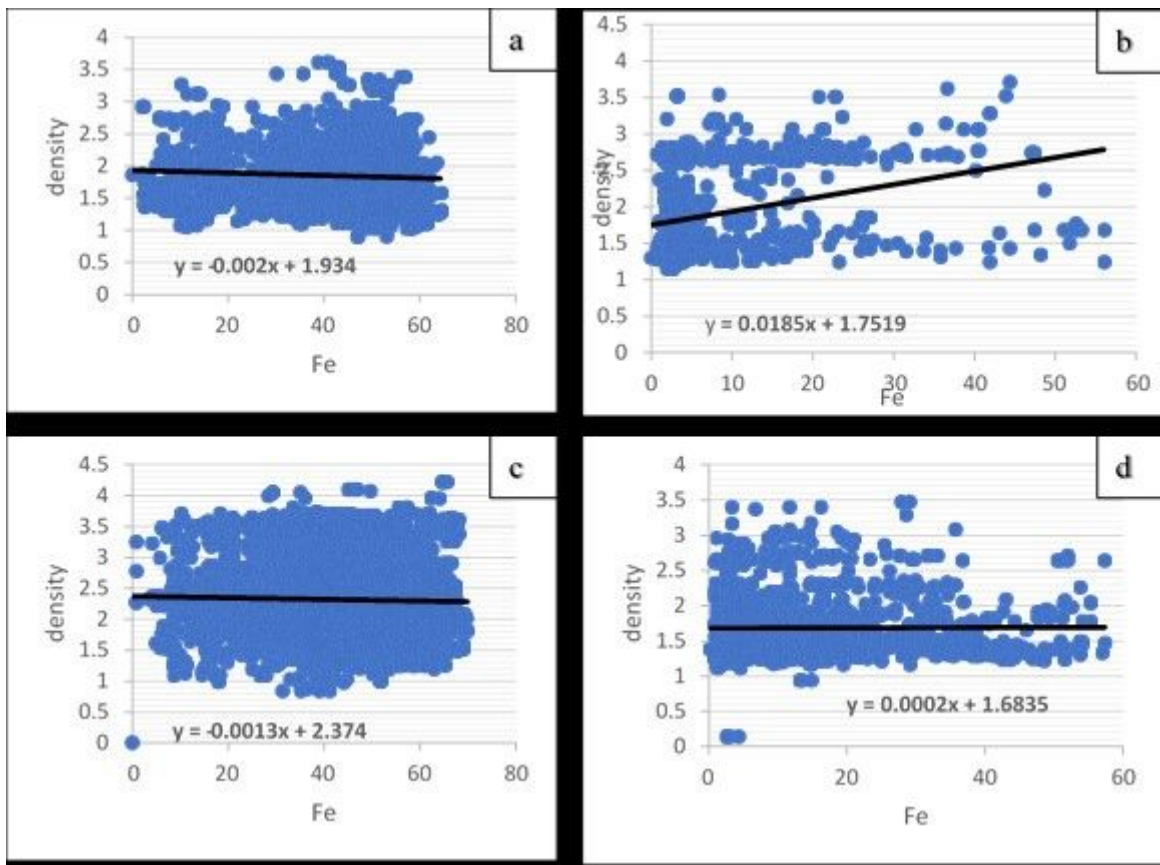


Figure 11

Density analysis for geological domains: a) D1; b) D2; c) D3 and d) D4.

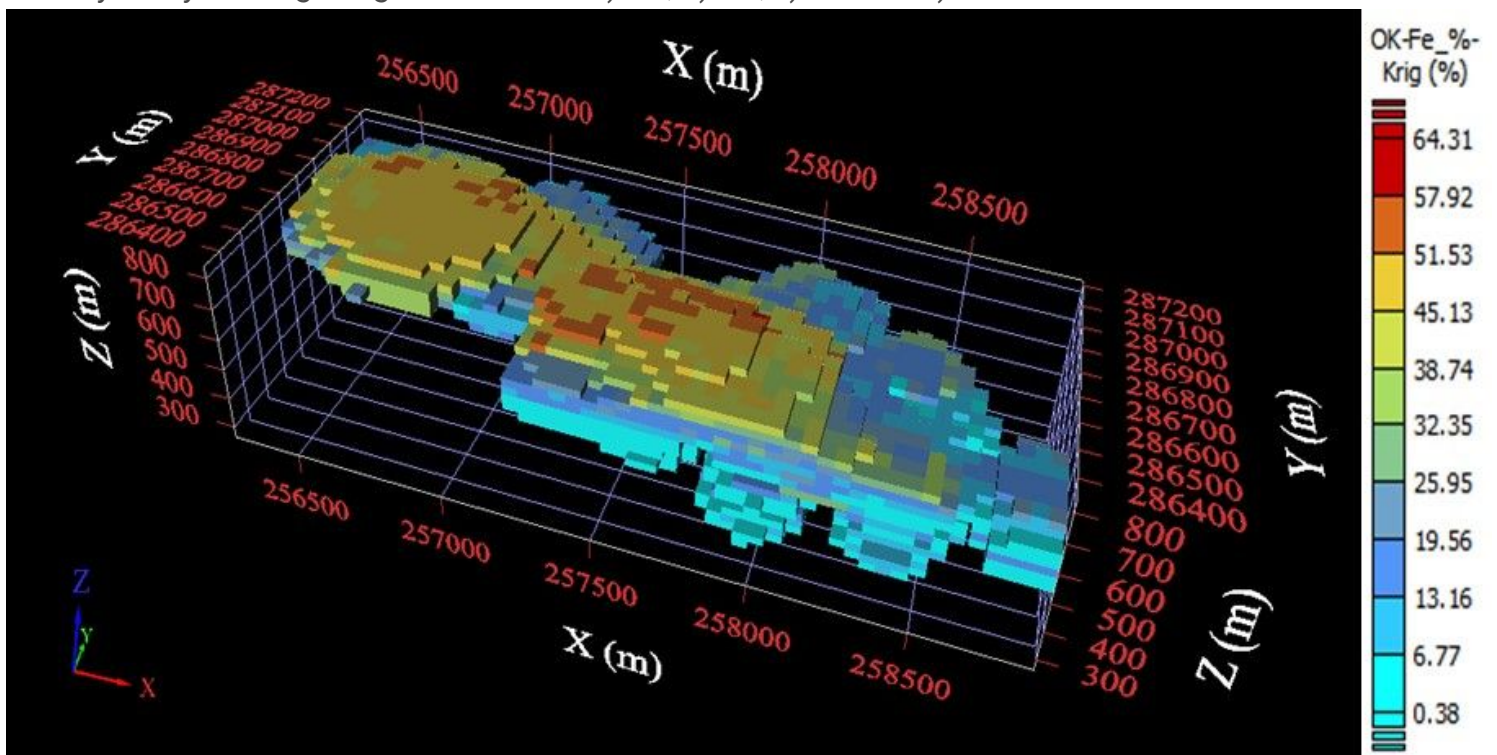


Figure 12

Block model of geochemical domain.

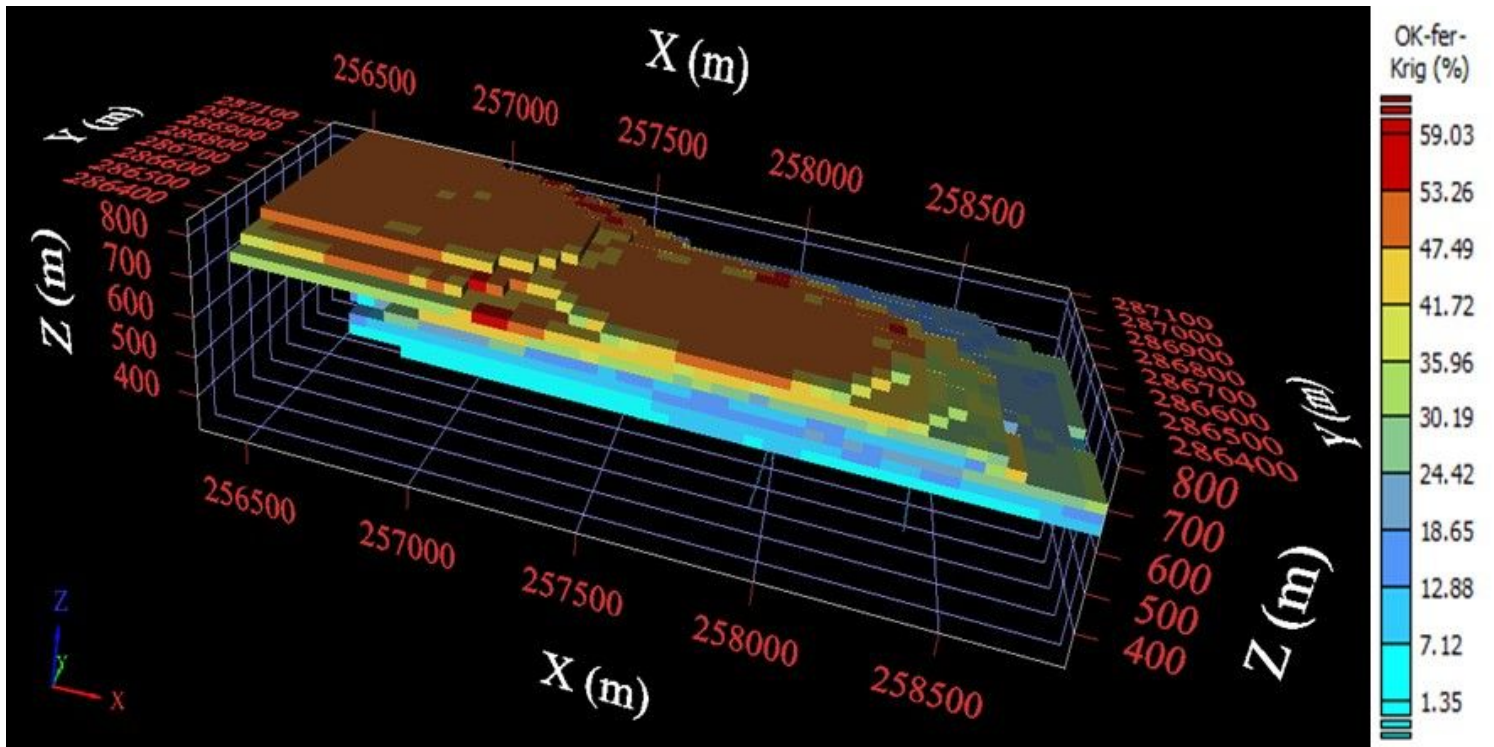


Figure 13

Block model of domain D1.

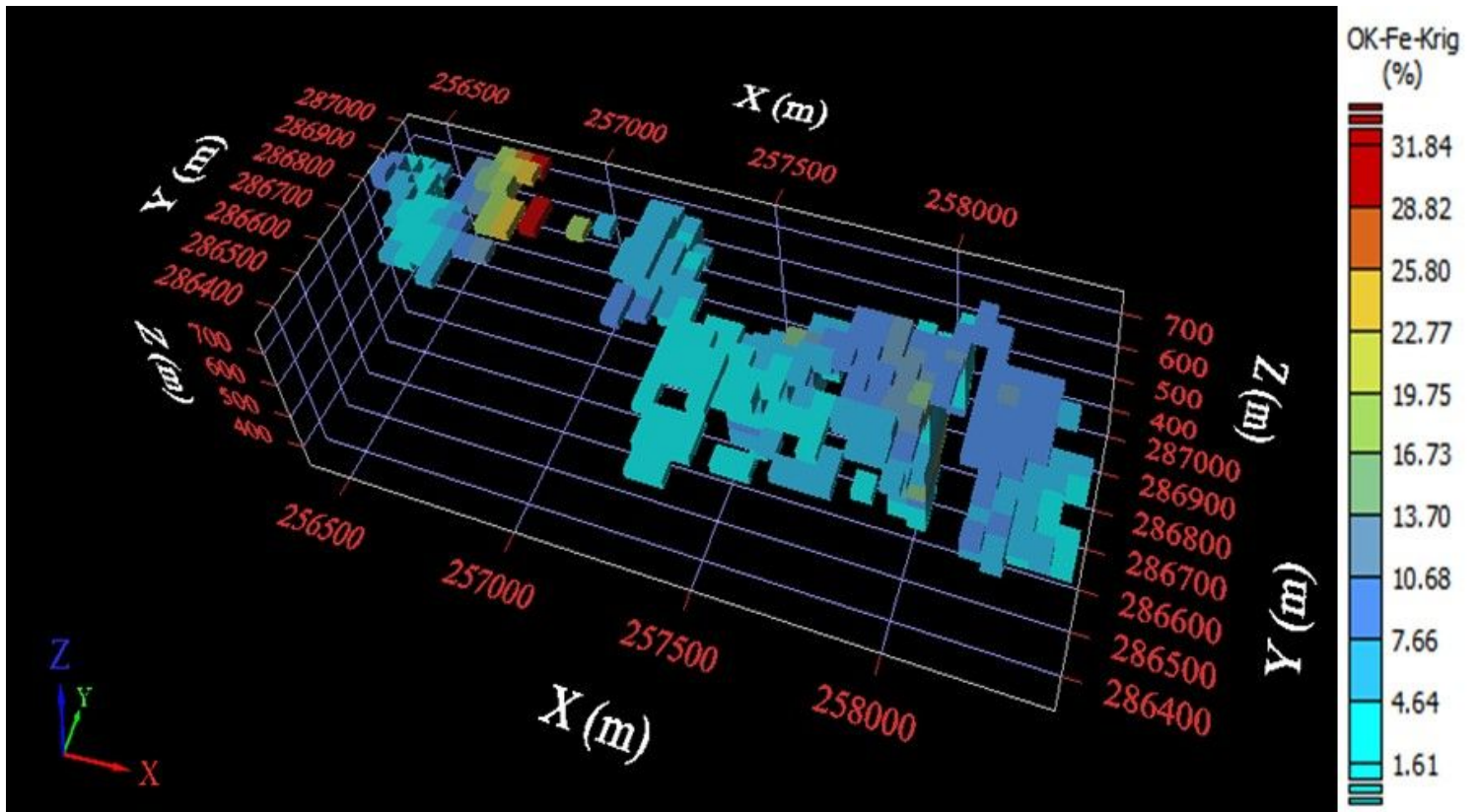


Figure 14

Block model of domain D2.

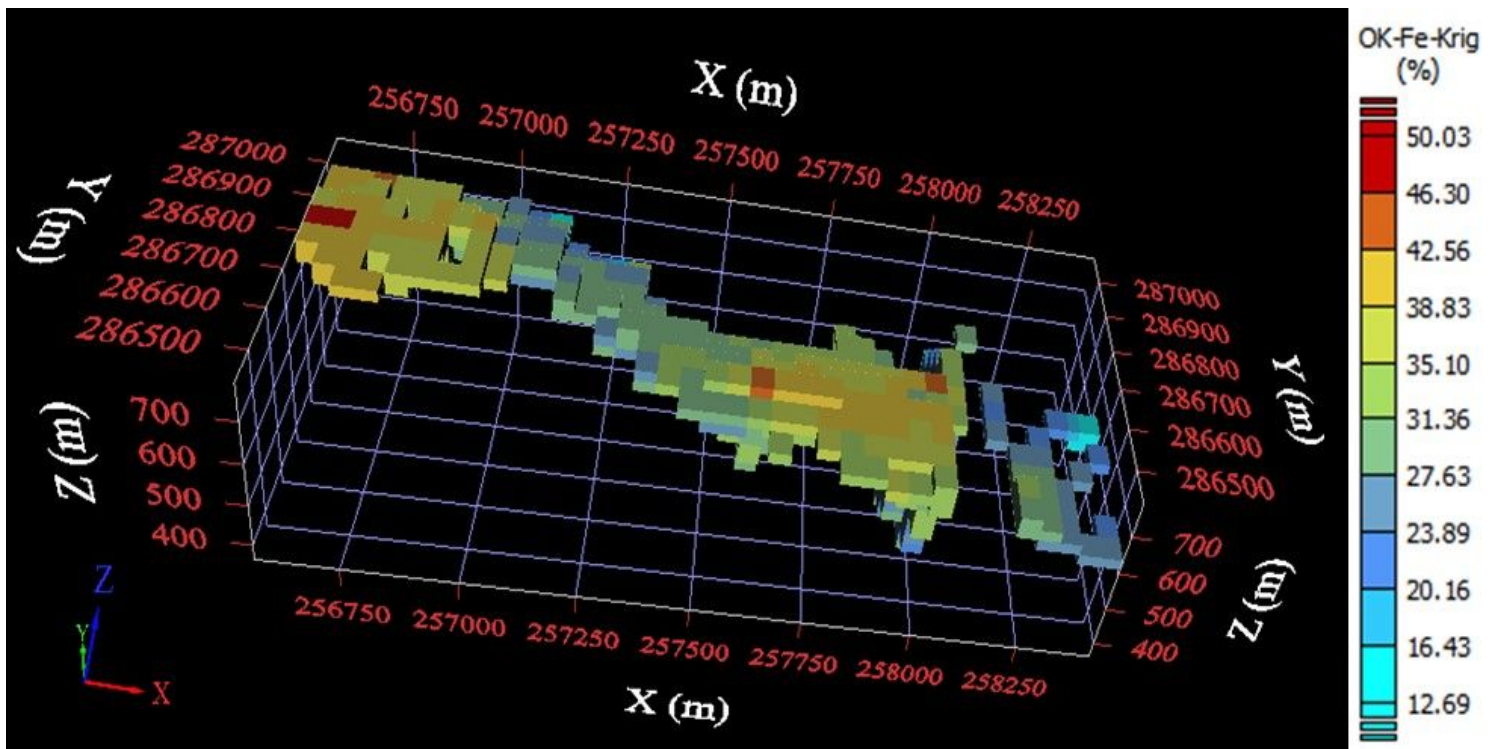


Figure 15

Block model of domain D3.

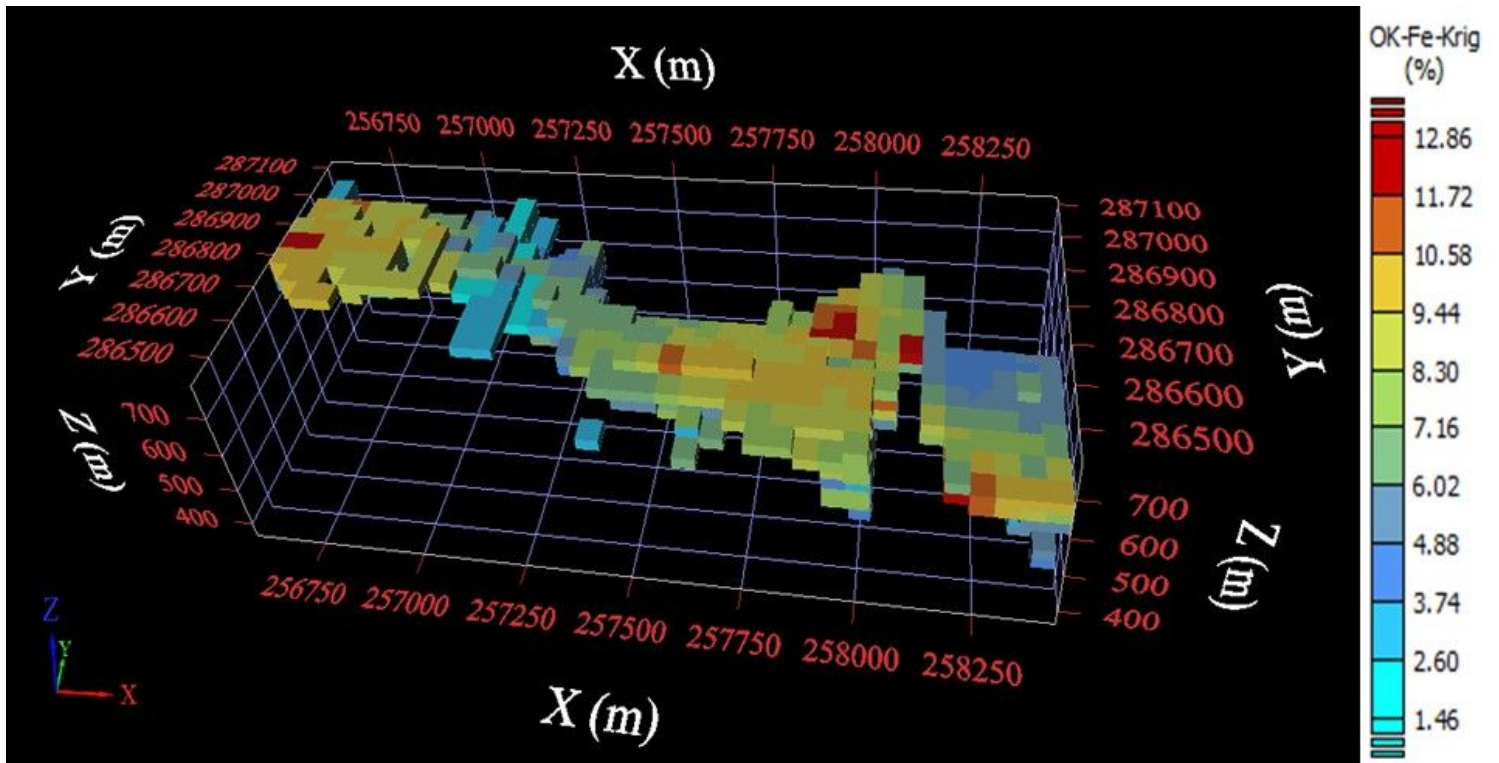


Figure 16

Block model of domain D4.

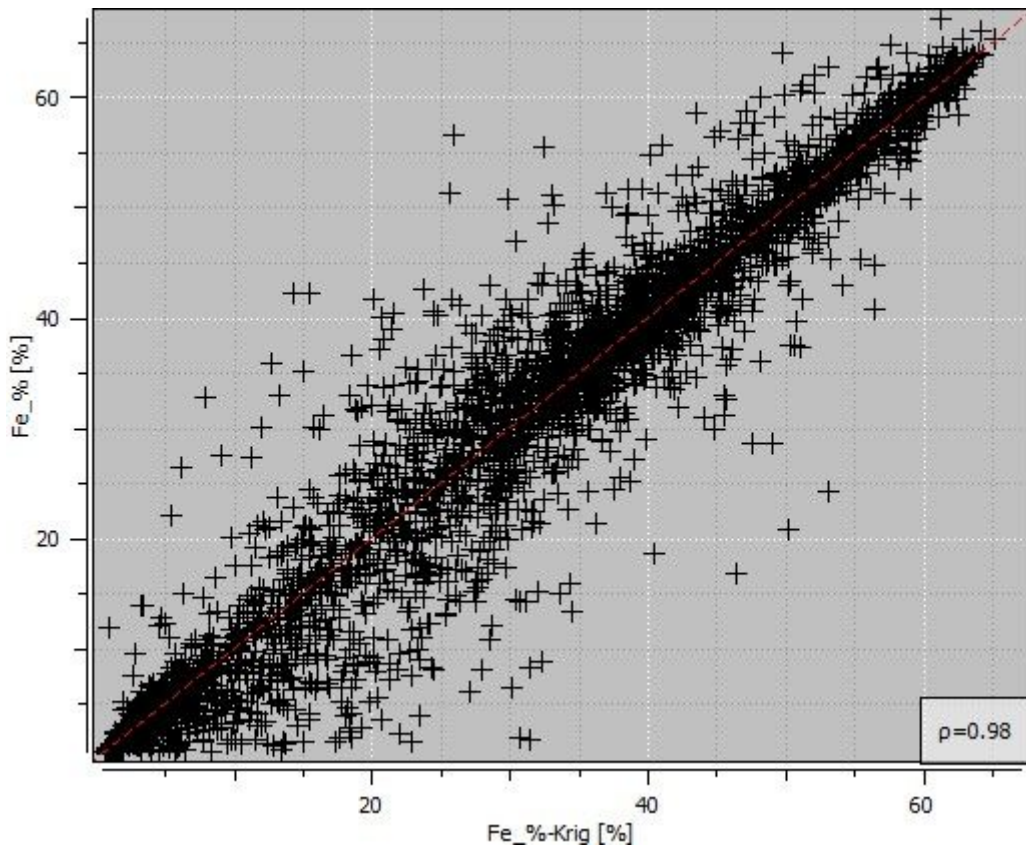


Figure 17

Cross-validation correlogram (global estimation).

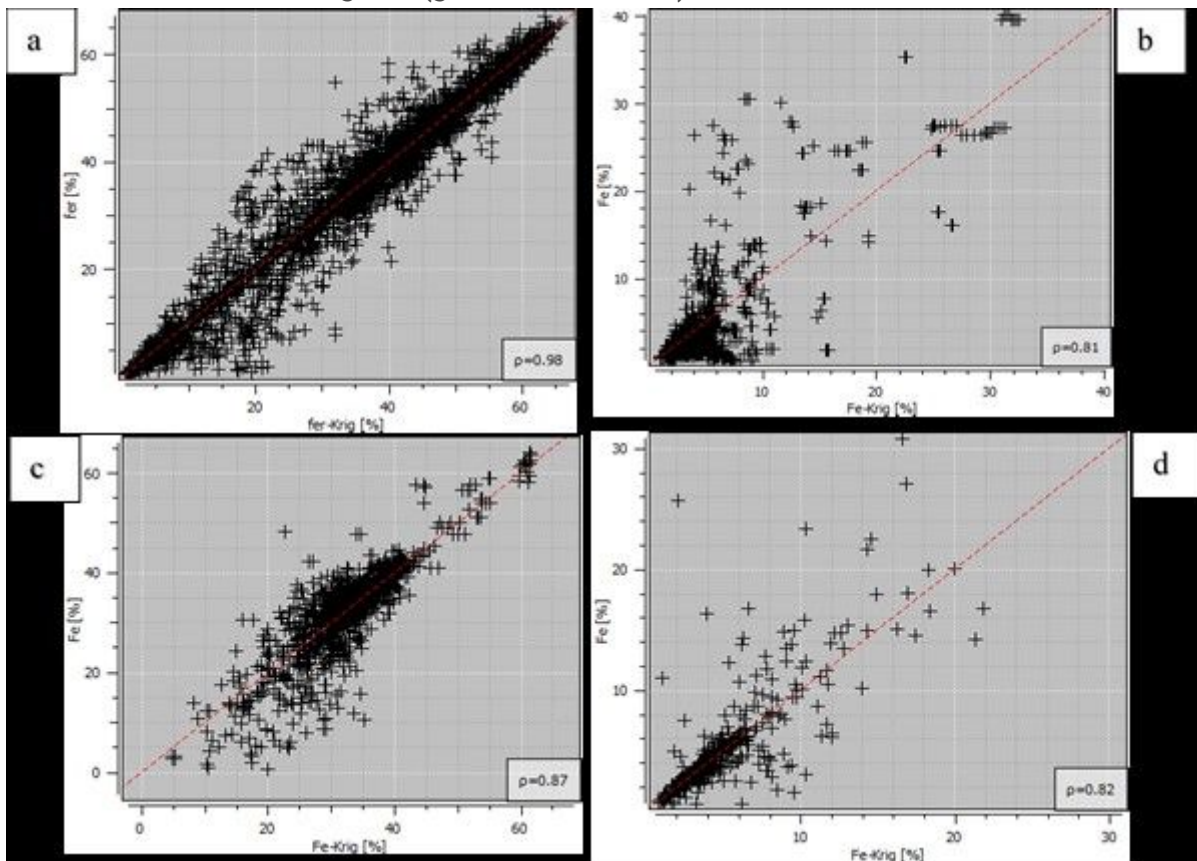


Figure 18

Cross-validation correlogram: a) D1; b) D2; c) D3 and d) D4.

Supplementary Files

This is a list of supplementary files associated with this preprint. Click to download.

- [Appendices.pdf](#)